SINTEF
PROCEEDINGS
2

Proceedings of the 12th International Conference on Computational Fluid Dynamics in the Oil & Gas, Metallurgical and Process Industries

Progress in Applied CFD – CFD2017

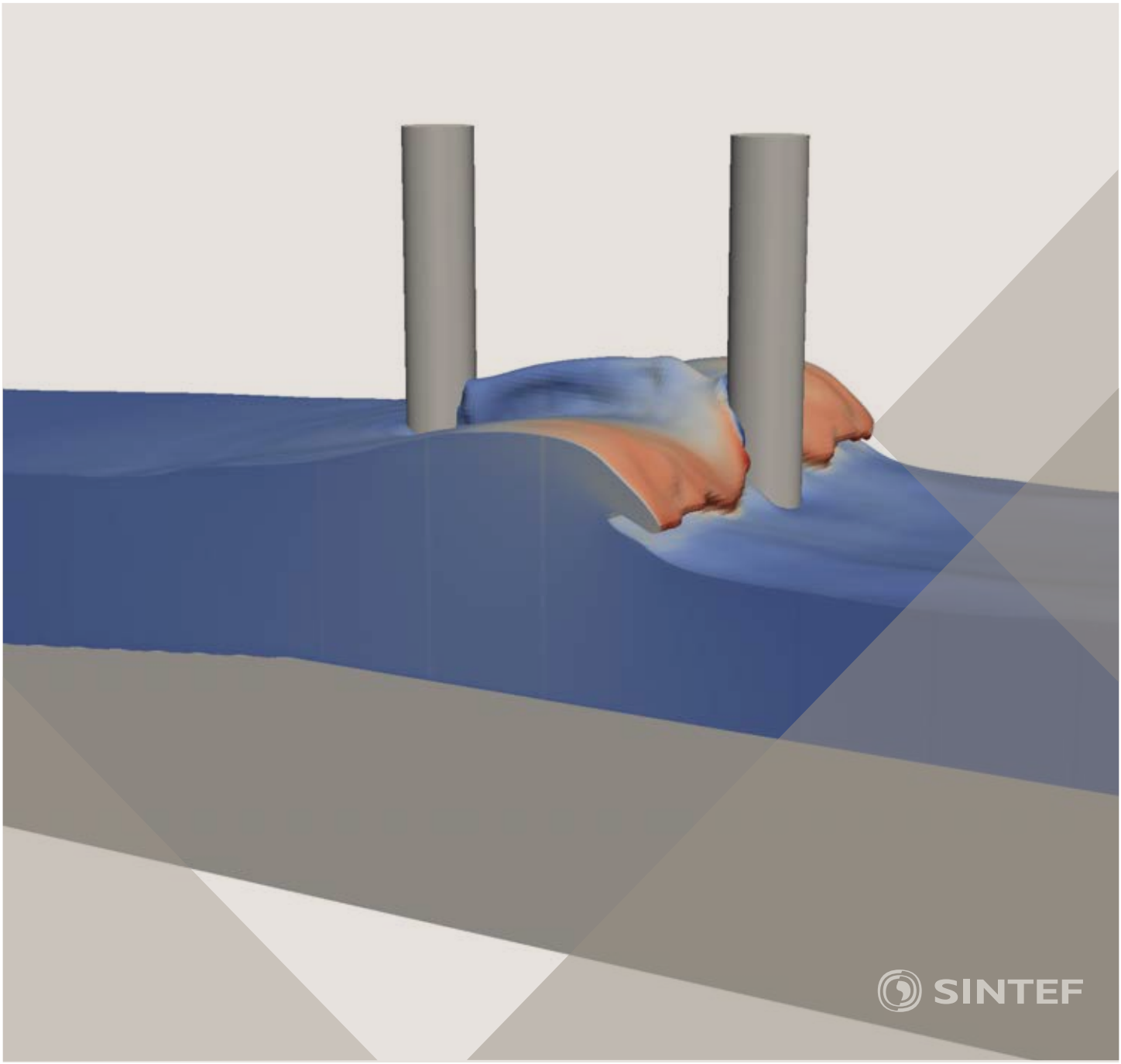

SINTEF Proceedings

Editors:
Jan Erik Olsen and Stein Tore Johansen

Progress in Applied CFD – CFD2017

Proceedings of the 12th International Conference on Computational Fluid Dynamics in the Oil & Gas, Metallurgical and Process Industries

SINTEF Academic Press

SINTEF Proceedings no 2
Editors: Jan Erik Olsen and Stein Tore Johansen
Progress in Applied CFD – CFD2017
Selected papers from 10th International Conference on Computational Fluid Dynamics in the Oil & Gas, Metallurgical and Process Industries

Key words:
CFD, Flow, Modelling

Cover, illustration: Arun Kamath

ISSN 2387-4295 (online)
ISBN 978-82-536-1544-8 (pdf)

SINTEF Academic Press
Address: Forskningsveien 3 B
PO Box 124 Blindern
N-0314 OSLO
Tel: +47 73 59 30 00
Fax: +47 22 96 55 08

www.sintef.no/byggforsk
www.sintefbok.no

SINTEF Proceedings
SINTEF Proceedings is a serial publication for peer-reviewed conference proceedings on a variety of scientific topics.
The processes of peer-reviewing of papers published in SINTEF Proceedings are administered by the conference organizers and proceedings editors. Detailed procedures will vary according to custom and practice in each scientific community.

PREFACE

This book contains all manuscripts approved by the reviewers and the organizing committee of the 12th International Conference on Computational Fluid Dynamics in the Oil & Gas, Metallurgical and Process Industries. The conference was hosted by SINTEF in Trondheim in May/June 2017 and is also known as CFD2017 for short. The conference series was initiated by CSIRO and Phil Schwarz in 1997. So far the conference has been alternating between CSIRO in Melbourne and SINTEF in Trondheim. The conferences focuses on the application of CFD in the oil and gas industries, metal production, mineral processing, power generation, chemicals and other process industries. In addition pragmatic modelling concepts and bio-mechanical applications have become an important part of the conference. The papers in this book demonstrate the current progress in applied CFD.

The conference papers undergo a review process involving two experts. Only papers accepted by the reviewers are included in the proceedings. 108 contributions were presented at the conference together with six keynote presentations. A majority of these contributions are presented by their manuscript in this collection (a few were granted to present without an accompanying manuscript).

The organizing committee would like to thank everyone who has helped with review of manuscripts, all those who helped to promote the conference and all authors who have submitted scientific contributions. We are also grateful for the support from the conference sponsors: ANSYS, SFI Metal Production and NanoSim.

Stein Tore Johansen & Jan Erik Olsen

Organizing committee:

Conference chairman: Prof. Stein Tore Johansen
Conference coordinator: Dr. Jan Erik Olsen
Dr. Bernhard Müller
Dr.Sigrid Karstad Dahl
Dr.Shahriar Amini
Dr.Ernst Meese
Dr.Josip Zoric
Dr.Jannike Solsvik
Dr.Peter Witt

Scientific committee:

Stein Tore Johansen, SINTEF/NTNU
Bernhard Müller, NTNU
Phil Schwarz, CSIRO
Akio Tomiyama, Kobe University
Hans Kuipers, Eindhoven University of Technology
Jinghai Li, Chinese Academy of Science
Markus Braun, Ansys
Simon Lo, CD-adapco
Patrick Segers, Universiteit Gent
Jiyuan Tu, RMIT
Jos Derksen, University of Aberdeen
Dmitry Eskin, Schlumberger-Doll Research
Pär Jönsson, KTH
Stefan Pirker, Johannes Kepler University
Josip Zoric, SINTEF

CONTENTS

A SIMULATION CONCEPT FOR GENERIC SIMULATION OF MULTI-MATERIAL FLOW USING STAGGERED CARTESIAN GRIDS

Ernst A. MEESE[1], **Stein T. JOHANSEN**[1,2*]

[1] SINTEF Materials and Chemistry, Trondheim, NORWAY
[2] Norwegian University of Science and Technology (NTNU), Trondheim, NORWAY

* Corresponding author, E-mail address: Stein.T.Johansen@sintef.no

ABSTRACT

Simulation of multiphase flows is generally treated by various classes of Eulerian methods, Lagrangian methods, and various combinations of these. In the SIMCOFLOW initiative, we have set out to develop a framework for simulation of multi-material flows, using a Eulerian description. A fundamental part is the application of Cartesian grids with cut cells, and with a staggered representation of the grid for velocities and scalars. The model equations are derived based on formal volume and ensemble averaging (Quintard and Whitaker, 1995), (Gray and Lee, 1977) and (Cushman, 1982). Solid walls or moving solid materials are treated in the same manner as any flowing material (fluid, deforming material). The interface is characterized by a level set or by a 3D surface. In grid cells that are cut by a large-scale interface, the stress acting at the cut surface can be computed based on the level set or volume fractions. The exchange of mass, energy, and momentum between continuous fluids (note: walls are also considered a continuous fluid) can be estimated using wall functions in the case of coarse grids. The methods applied to the flow in a general geometry are closely related to the FAVOR method (Hirt and Sicilian, 1985) and the LS-STAG method (Cheny and Botella, 2010).

In this paper, we discuss the derivation of the equations and the numerical solution strategy needed to handle such complex physics within the framework of finite volume methods.

We further discuss briefly the ongoing developments such as adaptive gridding and the computational framework.

The results of this work will end up as open source software.

Keywords: Multi-material flows, Cartesian cut-cells, staggered grid, volume averaging, dispersed fields, large scale interface

NOMENCLATURE

Greek Symbols

α	volume fraction
β	interface specific volume fraction (m)
ρ	density (kg/m^3)
ρ_l	intrinsic density of phase l (kg/m^3)
$\hat{\rho}^{k;l}$	extensive phase density (kg/m^3), $\hat{\rho}^{k;l} = \alpha^{k;l}\rho_l$
χ_p	multiphase compressibility factor
$\boldsymbol{\tau}$	viscous stress tensor (Pa)

Latin Symbols

$\mathbf{A}$	interfacial area vector (m^2)
$\mathbf{A}$	matrix, defined by Eqs. (55) and (56)
DU	defined by equation (64)
$\mathcal{F}_\mathbf{i}$	index set for cell faces of grid cell **i**
$\mathbf{g}$	gravity vector (m/s^2)
$K^{k;l}_{m;n}$	interface friction coefficient between velocity fields $m;n$ and $k;l$
LSI	Large Scale Interface
$\mathbf{n}$	normal vector to interface
p	pressure at end of time step (Pa)
S	generic source term
Δt	time step (s)
p'	pressure correction, $p' = p - p^0$ (Pa)
T	temperature (K)
T'	temperature correction, $T' = T - T^0$ (K)
$u^{k;l}$	field velocity of phase k, dispersed into phase l (m/s)
u^*	defined by equation (53)

Superscripts

0	previous time step
$k;l$	field k, submerged into phase l

Subscripts

i	multi-index for grid cells, e.g., **i** = (i,j,k)
k	generic index for grid cell faces
w	wall index

Other symbols

$\langle\ \rangle$	volume averaged

INTRODUCTION

In Computational Fluid Dynamics (CFD), a number of different technical and scientific elements must play

Figure 1: Oil boom operated in calm sea.

together to create powerful methods that reliably can simulate real world behaviour. Multiphase and multi-material flows are of the most complex flows, and here the development of models with predictive power is generally lagging behind single phase flow models. An exception in the multiphase domain is free surface flows, which has shown some impressive developments over the last decade.

In an attempt to answer to challenges in multiphase pipe flow, we developed the LedaFlow Q3D model (Laux et al., 2007). In this model, multiple coexisting continuous and disperse phases can be represented. However, the code was tailored for pipe flows and could not readily be extended to complex geometries. The Research Council of Norway has now supported further development of these concepts through the SIMCOFLOW project. The target for this development is to simulate the flow of air, oil, and water in an operated oil boom (see Figure 1), interacting dynamically with wind, waves and sea current. Here we have set out to develop an open source CFD code that can handle any moving interface problem, using Cartesian grids with local grid refinement. The discretization of the governing equations is made on staggered grids, where the velocity component cells are centred at the faces of the scalar (primary) cell faces. A Cartesian Cut-Cell approach is applied to represent the immersed boundaries (Cheny and Botella, 2010; Hirt and Sicilian, 1985). The justification for working with this particular concept is a) relative ease of implementing new physical models using finite volumes on a regular mesh, b) exploit more accurate interpolation of fluxes, also due to grid regularity, c) easy automation of grid generation for any geometries using the cut-cell concept, and d) staggered mesh provides a tighter pressure-velocity coupling than what can be obtained using co-located grids. Previously it was unsuccessfully attempted to implement the CDP (Compressible Disperse Phase) method (Johansen and Laux, 1995) using a co-located mesh. Based on that experience, dealing with granular flows, it turned out that a staggered arrangement ensured positive pressures for all solid fractions, while the co-located approach generated from time to time negative pressures that killed the simulations.

In this paper, we present a theoretical and numerical framework for this development. To limit the scope of this paper, we only discuss discretization on regular Cartesian meshes. However, work is in progress for establishing a dynamic mesh structure, based on a graded octree representation (i.e., a 2:1 balance so that neighbouring cells are at most one level apart in the tree). The aim is to apply dynamic grid refinement in regions of interest, such as close to walls and to fluid-fluid interfaces. Using local grid refinement in Cartesian meshes introduces the additional complexity of hanging nodes, i.e., a grid cell may have two (2D) or four (3D) neighbouring cells in either coordinate direction, or it may be a connected to a neighbour through only half (2D) or a quarter (3D) of the neighbour's cell face. Due to space limitations, these additional discretization complexities and the actual procedure for dynamic refinement are not discussed here. We will focus on the model formulations that can allow such complex simulations.

MODEL DESCRIPTION

Cut-cell approach based on formal volume averaging

In order to handle the complex multiphase flows referred to above, we need a mathematical and numerical framework that can handle both complex wall geometries and fluid-fluid interfaces. An attempt to do so is represented by the FAVOR method (Hirt and Sicilian, 1985). However, in our case we want to extend the method to handle multiphase flows with any number of dispersed fields and continuous phases, as well as moving or stationary solids.

For the sake of simplicity, in the first part of this paper we go through some fundamental concepts looking only at single phase flow, extending the method to multiphase flow in the latter part. The extension to generic multiphase flows is quite straightforward. The only new issue that will enter is that the moving fluids and fields are coupled through mass, momentum, and energy transfer. Stiffness due to these interactions can be handled locally in each cell using a fractional step approach, which is a very desirable feature for enabling good parallel performance of the simulation code.

Scalar transport

In order to familiarize ourselves with cut-cell related issues we start by investigating the evolution of enthalpy in a cut-cell domain. We investigate the conservation of enthalpy h where only conduction, convection, and simple energy sources S_h are allowed to change the enthalpy field.

It is assumed that the relation between enthalpy and temperature is known. Currently we assume that $h = C_p T$. Using the generic formalism ((Quintard and Whitaker, 1995), (Gray and Lee, 1977) and (Cushman, 1982)), a very simplified conservation of enthalpy that is sufficient to demonstrate the concepts can be expressed as,

$$\begin{aligned}\frac{\partial}{\partial t}\int_{V_f}\rho_f h dV \;=\; & -\int_{S_f}\rho_f h\mathbf{u}_f\cdot\mathbf{n}_f dS \\ & -\int_{A_w}\rho_k h\left(\mathbf{u}_f-\mathbf{u}_I\right)\cdot\mathbf{n}_{f,w}dS \\ & -\int_{S_f}\mathbf{q}\cdot\mathbf{n}_f dS-\int_{A_w}\mathbf{q}\cdot\mathbf{n}_f dS+\int_{V_f}\rho_f S_h dV\end{aligned} \tag{1}$$

where V_f is a fluid volume, S_f is the part of the volume surface interfacing a neighbouring fluid volume, and A_w

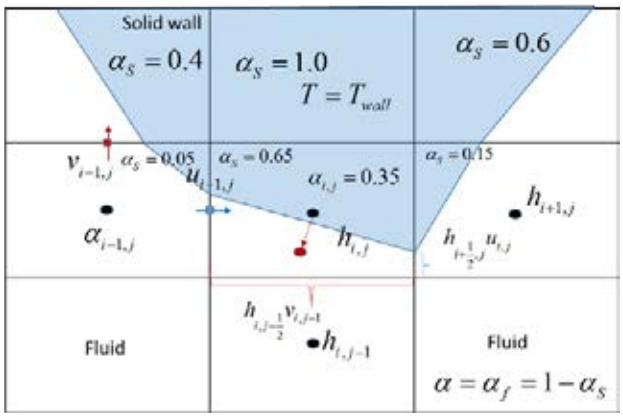

Figure 2 Cartesian cut cell domain with solid walls (blue) and enthalpy in cell (*i*,*j*) is $h_{i,j}$.

is the part of the volume surface interfacing a neighbouring solids region, see Figure 3.

The first term on the right hand side of Eq. (1) express the convection of enthalpy across cell faces, and the second term is the mass transfer between wall and fluid. RHS terms three and four express thermal conduction across the fluid cell boundary and into the solid wall, respectively. The last term is a general volumetric heat source.

The discrete enthalpy equations on a Cartesian grid cell **i** with fluid volume $V_f = \alpha_{f,\mathbf{i}} \Delta V_\mathbf{i}$ becomes,

$$\frac{\Delta\left(\alpha_f \rho_f h\right)_\mathbf{i}}{\Delta t}\Delta V_\mathbf{i} = -\sum_{\mathbf{k}\in\mathscr{F}_\mathbf{i}}\left(\rho_f h \mathbf{u}_f \cdot \mathbf{n}_f\, \alpha_f \Delta A\right)_\mathbf{k} - \sum_{\mathbf{k}\in\mathscr{F}_\mathbf{i}}\left(\mathbf{q}\cdot\mathbf{n}_f\, \alpha_f \Delta A\right)_\mathbf{k} - \sum_{\mathbf{w}\in\mathscr{W}_\mathbf{i}}\left(\mathbf{q}\cdot\mathbf{n}_f \Delta A\right)_\mathbf{w} + \int_{V_f}\rho_f S_h dV \quad (2)$$

where $\Delta(\alpha_f \rho_f h)_\mathbf{i}$ is the update of enthalpy over a time step, $\mathscr{F}_\mathbf{i}$ is the index set for the faces of cell **i**, and $\mathscr{W}_\mathbf{i}$ is the set of walls embedded in cell **i**. Note that we use a short-hand notation where the index of all variables inside parentheses is indicated on the parentheses itself.

In Eq. (2), the wall mass transfer term is absorbed into the generic source term. It is assumed that the velocity field is mass conserving. We will now discuss the implications of Eq. (2) when it comes to handling of the cut-cells.

Firstly, the transient term in Eq. (2) allows for a change in geometry, i.e., the solid fraction $\alpha_s = 1 - \alpha_f$ is changing between time steps.

For the convective term, i.e., the first term on the right hand side of Eq. (2), it becomes important that we have good estimates of the fluid fraction $(\alpha_f)_\mathbf{k}$ at cell boundaries. At the cell-face between cells $\mathbf{i} = (i,j)$ and $(i,j+1)$, the cell-face solid fraction in Figure 2 is clearly equal to one. If we compute the cell-face fraction by simple averaging, we have a situation where energy will flow between the two cells by conduction through the fluid phase. This is not acceptable. To avoid this problem, we have to introduce the following rules for cell interface fractions:

Rule I

A cell which is fully loaded by one phase will have that all the cell-face fractions of that phase is 1.

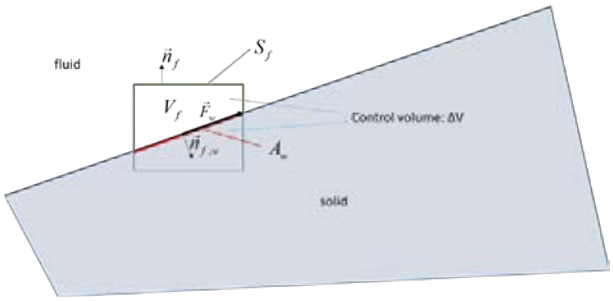

Figure 3 Control volume cut by solid. Force $\vec{F}_w$, acting on the fluid from the wall.

Rule II

A cell which have one, or more, but not all of the cell-faces dictated by Rule I will have a special method available to compute cell fractions for the remaining cell faces.

The values of the density ρ_f and enthalpy h_f at the cell-face that are needed to calculate the convective flux,

$$F_{\mathbf{k},\text{conv}} = \left(\rho_f h_f \mathbf{u}_f \cdot \mathbf{n}_f\, \alpha_f \Delta A\right)_\mathbf{k}, \quad (3)$$

are interpolated from neighbouring values using any preferred interpolation method. We note that the flux $F_{\mathbf{k},\text{conv}}$ is to be understood as the time averaged flux over the time step.

Wall treatment:

The wall flux is the generic transfer of heat between the fluid in the cell and the wall. The flux is generally treated as,

$$F_{\mathbf{w},\text{wall}} = \left(\mathbf{q}\cdot\mathbf{n}_f \Delta A\right)_\mathbf{w} = -\lambda \nabla T \cdot \mathbf{n}_\mathbf{w} \Delta A_\mathbf{w} = -\lambda \frac{T_{\mathbf{w},i,j} - T_{i,j}}{\delta_{\mathbf{w},n}} \Delta A_\mathbf{w} \quad (4)$$

Equation (4) can be replaced by wall functions in the case of turbulent flows.

Here λ is the thermal conductivity, $\Delta A_\mathbf{w}$ is the actual area (Rule III) of the wall cutting through the cell, and $\delta_{\mathbf{w},n}$ is the distance between the wall and the mass centre of the cell (Rule IV).

Rule III

The heat transfer area $\Delta A_\mathbf{w}$ of a cell cut by a wall is computed by a specific method (not detailed here).

Rule IV

The distance between a wall and the cell centre inside the fluid part of the cell is computed by a specific method. The first version of the method is based on computation of the mass centre in the fluid part of the cell and computation of the normal distance $\delta_{\mathbf{w},n}$ between this point and the cell-face.

The fluid conduction flux can be treated in a similar manner as for the convective fluxes. An example for the *x*-direction flux at the positive *x*-cell-face is,

$$F^{x^+}_{\mathbf{k},\text{cond}} = \left(q_x \cdot n_{f,x}\, \alpha_f \Delta A\right)^{x^+}_\mathbf{k} = -\left(\alpha_f \Delta A \lambda\right)^{x^+}_\mathbf{k} \frac{T_{i+i,j} - T_{i,j}}{\Delta x} \quad (5)$$

The computations and application of the cell interface fractions α_f are identical for conduction and convection. However, we note that due to Rule IV, the location point

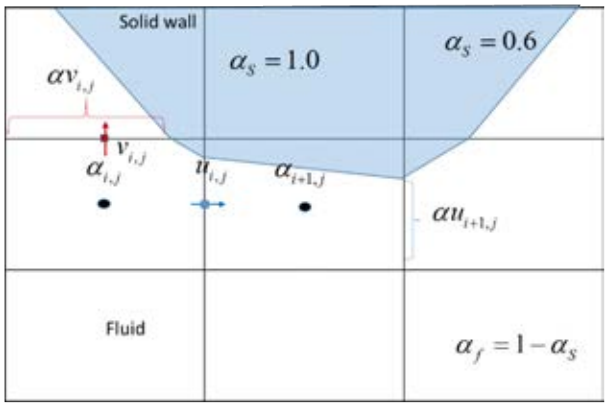

Figure 4 Staggered grid layout in 2D

for the temperature and enthalpy is moved from the cell centre to a new position (red circle in Figure 2). The movement of the point will impact the conductive fluxes across the neighbouring cell faces. It is therefore suggested that the offset of points in the cut cells are accounted for in the conductive flux calculations.

Rule V

The offset of cell centre points for a fluid in a cut cell is used to correct the diffusive exchange fluxes with neighbouring fluid cells.

Mass equations

According to the formalism (Cushman, 1982; Gray and Lee, 1977; Quintard and Whitaker, 1995) the transport equation for fluid mass is

$$\frac{\partial}{\partial t}\int_{V_f} \rho_f dV = -\int_{S_f} \rho_f \mathbf{u}_f \cdot \mathbf{n}_f dS - \int_{A_w} \rho_f \left(\mathbf{u}_f - \mathbf{u}_I\right)\cdot \mathbf{n}_{f,w} dS \,, \quad (6)$$

Referring again to Figure 3 for definition of V_f, S_f, and A_w. Integrating $\rho_f(\mathbf{x})$ over the fluid volume V_f we find the intrinsic average of the density. The fluid mass per volume in a grid cell may then be defined as

$$\hat{\rho} = \alpha_f \rho_f = \left(1-\alpha_S\right)\rho_f \,, \quad (7)$$

where α_f and α_s are the fluid and solids fraction (solid wall fraction) respectively, and $\rho_f = \rho(p,T)$ is the intrinsic density of the fluid phase.

For a grid cell with volume $\Delta V_\mathbf{i}$, we may write the discrete mass equation as

$$\frac{\partial \hat{\rho}_\mathbf{i}}{\partial t}\Delta V_\mathbf{i} + \sum_{\mathbf{k}\in\mathscr{F}_\mathbf{i}} \left(\hat{\rho}\,\mathbf{u}_f \cdot \mathbf{n}\Delta A\right)_\mathbf{k} = -\rho_f\left(\mathbf{u}_f - \mathbf{u}_I\right)\mathbf{n}_{f,w}\Delta A_w \quad (8)$$

Note that the term on the right hand side of Eq. (8) may represent both a flow (mass source) coming through the wall, or any combination with an interface moving with velocity $\mathbf{u}_I$.

If the solid (walls, external domain) is stationary the mass equation will simplify to,

$$\frac{\partial \hat{\rho}_\mathbf{i}}{\partial t}\Delta V_\mathbf{i} + \sum_{\mathbf{k}\in\mathscr{F}_\mathbf{i}} \left(\hat{\rho}\,\mathbf{u}_f \cdot \mathbf{n}\Delta A\right)_\mathbf{k} = S_\mathbf{i} \quad (9)$$

where $S_\mathbf{i}$ is a generic source term in cell **i**. In Figure 4, we see a typical staggered grid layout in 2D that is used to construct the discretization.

Momentum equations

The momentum equation over a fluid volume V_f may be formulated as,

$$\begin{aligned}\frac{\partial}{\partial t}\int_{V_f} \rho\mathbf{u} dV &= \int_{V_f} \rho\mathbf{g} dV \\ &+ \int_{S_f} \left(-p\mathbf{I}+\boldsymbol{\tau}\right)\cdot\mathbf{n}_f dS + \int_{A_w} \left(-p\mathbf{I}+\boldsymbol{\tau}\right)\cdot\mathbf{n}_{f,w} dS \\ &- \int_{S_f} \rho\mathbf{u}\mathbf{u}\cdot\mathbf{n}_f dS - \int_{A_w} \rho\mathbf{u}\left(\mathbf{u}-\mathbf{u}_I\right)\cdot\mathbf{n}_{f,w} dS\end{aligned} \quad (10)$$

For the volume integrals at the top line of Eq. (10), we have for grid cell **i**, where $V_f = \alpha_{f,\mathbf{i}}\Delta V_\mathbf{i}$, that

$$\frac{\partial}{\partial t}\int_{V_f} \rho\mathbf{u} dV = \frac{\partial \hat{\rho}_\mathbf{i}\mathbf{u}_\mathbf{i}}{\partial t}\Delta V_\mathbf{i} \text{ and } \int_{V_f} \rho\mathbf{g} dV = \hat{\rho}_\mathbf{i}\mathbf{g}\Delta V_\mathbf{i} \,, \quad (11)$$

where the values $\hat{\rho}_\mathbf{i}$ and $\mathbf{u}_\mathbf{i}$ on the right hand sides are volume averaged magnitudes over V_f, and $\hat{\rho}_\mathbf{i}$ is defined as in Eq. (7).

For the stress terms, we have that

$$\int_{S_f} \left(-p\mathbf{I}+\boldsymbol{\tau}\right)\cdot\mathbf{n}_f dS = \sum_{\mathbf{k}\in\mathscr{F}_\mathbf{i}} \left[\left(-p\mathbf{I}+\boldsymbol{\tau}\right)\cdot\mathbf{n}\,\alpha_f\Delta A\right]_\mathbf{k} \quad (12)$$

and for wall stresses,

$$\int_{A_w} \left(-p\mathbf{I}+\boldsymbol{\tau}\right)\cdot\mathbf{n}_{f,w} dS) = \left(-p\mathbf{I}+\boldsymbol{\tau}\right)_\mathbf{w}\cdot\mathbf{n}_{f,\mathbf{w}}\Delta A_\mathbf{w} \quad (13)$$

The advection term becomes

$$\int_{S_f} \rho\mathbf{u}\mathbf{u}\cdot\mathbf{n}_f dS = \sum_{\mathbf{k}\in\mathscr{F}_\mathbf{i}} \left(\rho\mathbf{u}\mathbf{u}\cdot\mathbf{n}\,\alpha_f\,\Delta A\right)_\mathbf{k} \quad (14)$$

Note that all variables on the right-hand sides of Eqs. (12) – (14) are face-averaged values, so that no approximations have been made yet.

To arrive at a discretization of Eq. (10), several interesting observations can be made.

i) The surface averages of pressure in the stress terms (12) and (13) can be approximated closely by the volume averages.

ii) For the stress term in Eq. (12), some cell faces may have zero fluid fraction ($\alpha_{f,\mathbf{k}} = 0$). The contribution from these cell faces will disappear for the pressure and the shear stress.

iii) The wall effect is reintroduced by the stress term in Eq. (13). The stress contribution will have to be computed based on the surrounding discrete velocity values and volume fractions. In addition, the pressure contribution here involves only the pressure internally in the fluid in the cell, not a pressure behind the interface. As a consequence of ii) and iii) there will be no fluid pressure (and no need for it) in a cell which is fully solid.

iv) The transfer term

$$\int_{A_w} \rho\mathbf{u}\left(\mathbf{u}-\mathbf{u}_I\right)\cdot\mathbf{n}_{f,w} dS$$

will only have values for the case where mass is entering or leaving through the wall face. In the case of an inert wall surface, moving through space, we will have zero contribution from this term. This applies to typical fluid-structure interaction cases.

Treatment of wall boundary conditions

In Figure 3 we see the wall shear force $\vec{F}_w$ acting on the fluid in the volume V_f. The shear force acts in the direction of the fluid velocity, tangential to the wall. The wall may have any velocity $\mathbf{u}_w$. First we need the relative velocity between the fluid and the wall, tangential to the

wall. The relative velocity vector $\Delta\mathbf{u}$ between the fluid and the wall is,

$$\Delta\mathbf{u} = \mathbf{u} - \mathbf{u}_\mathbf{w} \tag{15}$$

so that the relative velocity normal to the wall is,

$$\Delta\mathbf{u}_n = \left[\left(\mathbf{u} - \mathbf{u}_\mathbf{w}\right)\cdot\mathbf{n}\right]\mathbf{n} \tag{16}$$

where $\mathbf{n}$ is the unit vector normal to the wall. The relative velocity tangential to the wall is then,

$$\Delta\mathbf{u}_t = \Delta\mathbf{u} - \Delta\mathbf{u}_n = \Delta\mathbf{u} - \left[\Delta\mathbf{u}\cdot\mathbf{n}\right]\mathbf{n} \tag{17}$$

The unit normal vector for the relative flow, parallel to the wall in now,

$$\mathbf{n}_t = \frac{\Delta\mathbf{u}_t}{\left|\Delta\mathbf{u}_t\right|} = \frac{\Delta\mathbf{u} - \left[\Delta\mathbf{u}\cdot\mathbf{n}\right]\mathbf{n}}{\left|\Delta\mathbf{u} - \left[\Delta\mathbf{u}\cdot\mathbf{n}\right]\mathbf{n}\right|} \tag{18}$$

The force acting on the fluid at a wall will be in the direction of $\mathbf{n}_t$ and can be given as,

$$\vec{F}_w = -\left|\tau_w\right| A_w \mathbf{n}_\mathbf{t} \tag{19}$$

The wall force decomposed into each Cartesian coordinate direction can now be written as,

$$\begin{aligned} F_{w,x} &= -\left|\tau_w\right| A_w \mathbf{n}_\mathbf{t}\cdot\mathbf{e}_\mathbf{x} \\ F_{w,y} &= -\left|\tau_w\right| A_w \mathbf{n}_\mathbf{t}\cdot\mathbf{e}_y \\ F_{w,z} &= -\left|\tau_w\right| A_w \mathbf{n}_\mathbf{t}\cdot\mathbf{e}_z \end{aligned} \tag{20}$$

In the case of no flow, a tangential vector is easily computed from the cross product of any of base vectors which are not parallel with the normal vector.

For the stability of a numerical implementation without having to excessively limit the time step size, it is critical to linearize the wall stress in velocity for use in an implicit scheme for the viscous terms. This is done in the following (example for Cartesian x-direction). The wall stress is Taylor-expanded in the required direction, here x-direction,

$$\left|\tau_w\right| \approx \left|\tau_w\right|^0 + \left(\frac{\partial\left|\tau_w\right|}{\partial\left|\Delta\mathbf{u}_t\right|}\frac{\partial\left|\Delta\mathbf{u}_t\right|}{\partial\Delta u_{t,x}}\right)^0 \left(\Delta u_{t,x} - \Delta u^0_{t,x}\right) \tag{21}$$

We use the wall function concept, stating that,

$$\left|\Delta\mathbf{u}_t(y)\right| = u_\tau u^+(y^+), \tag{22}$$

where u_τ is the friction velocity, u^+ the velocity normalized by the friction velocity, and y^+ the normalized wall distance. Eq. (22) is equivalent to,

$$\left|\tau_w\right| = \rho u_\tau^{\,2} = \rho\left(\frac{\left|\Delta\mathbf{u}_t(y)\right|}{u^+(y^+)}\right)^2 \tag{23}$$

Using (23) in (21) we have that,

$$\left|\tau_w\right| \approx \left|\tau_w\right|^0 + \left\{\frac{2\left|\tau_w\right|}{\left|\Delta\mathbf{u}_t\right|}\frac{\Delta u_{t,x}}{\left|\Delta\mathbf{u}_t\right|}\right\}^0 \left(\Delta u_{t,x} - \Delta u^0_{t,x}\right) \tag{24}$$

We may now write the viscous stress, linearized in the fluid and wall velocities in the x-direction, as

$$\begin{aligned} \left|\tau_w\right| \approx & \underbrace{\left|\tau_w\right|^0 - \left\{\frac{2\left|\tau_w\right|}{\left|\Delta\mathbf{u}_t\right|}\frac{\Delta u_{t,x}}{\left|\Delta\mathbf{u}_t\right|}\right\}^0 \Delta u^0_{t,x}}_{\tau_A} \\ & + \underbrace{\left\{\frac{2\left|\tau_w\right|}{\left|\Delta\mathbf{u}_t\right|}\frac{\Delta u_{t,x}}{\left|\Delta\mathbf{u}_t\right|}\right\}^0}_{\chi}\left(u_x - u_{w,x}\right) \\ = & \tau_A + \chi\left(u_x - u_{w,x}\right) \end{aligned} \tag{25}$$

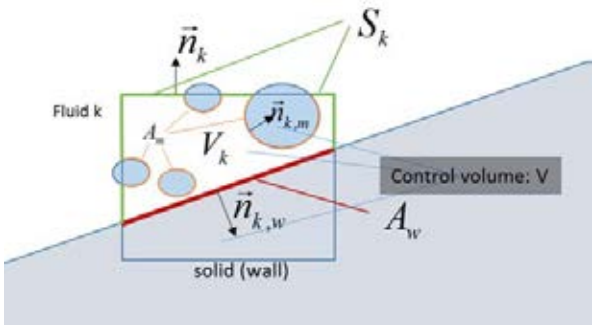

Figure 5 Control volume *V*, containing field *k*, cut by solid (or fluid-fluid interface), and by dispersed fields *m*.

The x-direction force can in turn be written as

$$F_{w,x} = -\tau_A n_{t,x}\Delta A_w - \chi n_{t,x}\left(u_x - u_{w,x}\right)\Delta A_w \tag{26}$$

Test: Flow parallel to wall. $n_y = 1$, $n_{t,x} = 1$, $u_w = 0.0$ m/s:

$$\left|\tau_w\right| \approx -\underbrace{\left|\tau_w\right|^0}_{\tau_A} + \underbrace{\left\{\frac{2\left|\tau_w\right|}{\left|\Delta\mathbf{u}_t\right|}\right\}^0}_{\chi} u_x \tag{27}$$

The resulting force is:

$$F_{w,x} = \left(\left|\tau_w\right|^0 - \frac{2\left|\tau_w\right|^0}{\left|\Delta\mathbf{u}_t\right|^0}u_x\right)\Delta A_w \tag{28}$$

This result is as expected. Note that due to the properties of Eq. (23), the linearization factor becomes $\frac{2\left|\tau_w\right|^0}{\left|\Delta\mathbf{u}_t\right|^0}$ and not $\frac{\left|\tau_w\right|^0}{\left|\Delta\mathbf{u}_t\right|^0}$!

MULTIPHASE FLOW EQUATIONS

We now introduce multiple phases and the fields used to represent them (Laux et al., 2007). We use notation $\alpha^{k;l}$ to tell that this is the volume fraction of a field with index k that is submerged in a phase l. The continuous field for phase l is denoted as $\alpha^{l;l}$. The field velocity is $u^{k;l}$, and accordingly the continuous phase velocity is $u^{l;l}$.

In order to support the functionality that only some fields are active in various parts of the solution domain, we may apply a field indicator $\Upsilon^{k;l}$, where

$$\Upsilon^{k;l} = \begin{cases} 1 & \text{if field } k \text{ in phase } l \text{ exists} \\ 0 & \text{if field } k \text{ in phase } l \text{ is non-existing} \end{cases}, \tag{29}$$

For convenience, in the computer code we may attach string tables to the indices, where the entries in the table could be, e.g., ["gas","oil","water","sand","wall_1"]. The pair $(k;l) = (1;2)$ would then refer to dispersed gas in the oil phase. In this notation, $k = l$ represents the case where the field is the continuous phase. I.e., in our example, all fields carried by the continuous water phase are represented by $\alpha^{k;3}$, continuous water is $\alpha^{3;3}$, gas bubbles in water is $\alpha^{1;3}$, and sand particles in water is $\alpha^{4;3}$. Since sand cannot be a continuous phase, we will have that $\Upsilon^{4;4} = 0$, and accordingly $\alpha^{4;4}$ do not exist. In this example, we have only one wall type, represented by wall fraction $\alpha^{5;5}$, and where $\Upsilon^{5;5} = 1$ and $\Upsilon^{i<5;5} = 0$.

Note also that the total number of fields in our system is given by

$$N_{\text{fields}} = \sum_{l=1}^{N_{\text{phases}}} \sum_{k=1}^{N_{\text{phases}}} \Upsilon^{k;l} \tag{30}$$

Special interface notation

For interfaces, we will use a special notation which handle the precise situation. We use the following notation, exemplified by the interfacial area:

$$A_{k;m\uparrow m;m}$$

Here the area is represented at the interface between field k submerged into phase m (k;m) and the continuous field (m;m). For dispersed fields, we may use the shortcut $A_{k;m\uparrow m;m} \equiv A_{k;m}$ without loss of generality. However, for continuous fields, having an interface between (k;k) and (m;m) we have to apply $A_{k;k\uparrow m;m}$ since $A_{k;k\uparrow m;m} \neq A_{k;m}$.

Multiphase mass equations

To arrive at the formal transport equation for mass we, as for single phase above, use the formalism provided in ((Quintard and Whitaker, 1995), (Gray and Lee, 1977) and (Cushman, 1982)). The transport equation for the mass of a field k, submerged in continuous phase m, can then be formulated as,

$$\begin{aligned}\frac{\partial}{\partial t}\int_{V^{k;m}} \rho^{k;m} dV = &-\int_{S_k} \rho^{k;m}\mathbf{u}^{k;m}\cdot\mathbf{n}^{k;m} dS \\ &\underbrace{-(1-\delta_{km})\int_{A_{k;m\uparrow m;m}} \rho^{k;m}\left(\mathbf{u}^{k;m}-\mathbf{u}_{I,k;m\uparrow m;m}\right)\cdot\mathbf{n}_{k;m\uparrow m;m} dS}_{\text{k is dispersed in m}} \\ &\underbrace{-\delta_{km}\sum_{j=1}^{L}\int_{A_{m;m\uparrow j;m}} \rho^{m;m}\left(\mathbf{u}^{m;m}-\mathbf{u}_{I,m;m\uparrow j;m}\right)\cdot\mathbf{n}_{m;m\uparrow j;m} dS}_{\text{j is dispersed in m}}\end{aligned} \tag{31}$$

Here the summation over j includes all dispersed fields present in the control volume. The Kronecker delta

$$\delta_{km} = \begin{cases} 0 & \text{if } k \neq m \\ 1 & \text{if } k = m \end{cases} \tag{32}$$

is introduced to select the correct form of the equations for continuous phases and non-continuous phases. The first term on the right-hand side of Eq. (31) accounts for mass leaving or entering the control volume. The two other terms correspond to mass transfer terms and will be non-zero only if the fluid velocity is different from the interface velocity.

In general, all walls are treated as a phase or field which is stationary or moving. In this way, there is no difference in the treatment of fluid-fluid, fluid-solid, or solid-solid interfaces. This will allow for any dynamics of the "solids".

Areas, volumes, and vectors are handled as discussed in the single-phase section and as explained in Figure 5, which sketches a typical multiphase situation. In Figure 5, the field marked as "wall" could be any continuous field, represented by a volume fraction $\alpha^{k;k}$ and a velocity $\mathbf{u}^{k;k}$. The dispersed field denoted m could be a collection of different fields.

The mass transfer terms in Eq. (31) involves sub-grid velocities, and will typically be modelled by source terms that will be specific to different mechanisms for mass transfer. For the discussion in this paper, we introduce a generic volumetric source term $S^{k;m}$ to represent these models for net mass transfer into field (k;m).

When we now integrate over the fluid volume $V^{k;m}$ we find the intrinsic average of the density. Using $\alpha^{k;m}$ as field fraction of the control volume, the field mass per volume in the complete control volume is

$$\hat{\rho}^{k;m} = \alpha^{k;m}\rho^{k;m}.$$

Here, $\rho^{k;m}(p,T)$ is the intrinsic density of the field phase, or rather of the phase labelled k since the fields represent subsets of all mass there is of a phase, where the thermodynamic properties, such as density, belongs to the phase.

The mass equation for the field ($\underline{k}$;m) on a Cartesian grid cell with index **i** can now be written as,

$$\frac{\partial \hat{\rho}_{\mathbf{i}}^{k;m}}{\partial t}\Delta V_{\mathbf{i}} + \sum_{\mathbf{k}\in\mathscr{F}_{\mathbf{i}}}\left(\hat{\rho}^{k;m}\,\mathbf{u}^{k,m}\cdot\mathbf{n}\,\Delta A\right)_{\mathbf{k}} = S_{\mathbf{i}}^{k;m}\Delta V_{\mathbf{i}} \tag{33}$$

where $\hat{\rho}_{\mathbf{i}}^{k;m}$ is mass per volume in the cell, the values of $\hat{\rho}$ and $\mathbf{u}\cdot\mathbf{n}$ in the parenthesis under the sum are average values over the cell faces, and **n** is the outward unit normal at the cell face.

Volume constraint

For multiphase flows, we get an algebraic constraint for volume that has to be fulfilled. It is stating that the sum of the volume occupied by all fields must equal the total available volume. I.e., the volume fractions have to fulfil the condition,

$$\sum_{m=1}^{N_{\text{phases}}}\sum_{k=1}^{N_{\text{phases}}} \Upsilon^{k;\mathrm{m}}\alpha^{k;\mathrm{m}} = 1 \tag{34}$$

Note that we have used the field indicator (29) to exclude fields that are not present in the model. At this stage we note that we in Eq. (34) have a total of N_{phases} different phases and types of walls, where these may have different appearances, but they are each represented by a field.

Multiphase momentum equations

Dispersed fields and single continuous fields in a grid cell

By following the suggestions above we arrive at the following momentum equation for a field k;l. The field k;l may be a continuous field containing other dispersed fields or a dispersed field submerged into a continuous filed. At this point we do not consider multiple continuous fields with-in a single grid cell. In addition, the considered flow is laminar. Turbulence may later be introduced by one more layer of ensemble averaging of the model equations.

$$
\begin{aligned}
&\frac{\partial}{\partial t}\left(\alpha^{k;l}\rho^{k;l}\mathbf{u}^{k;l}\right)+\nabla\cdot\left(\alpha^{k;l}\rho^{k;l}\left(\overline{\delta\mathbf{u}^{k;l}\delta\mathbf{u}^{k;l}}+\mathbf{u}^{k;l}\mathbf{u}^{k;l}\right)\right)\\
&\quad=\alpha^{k;l}\rho^{k;l}\mathbf{g}+\alpha^{k;l}\nabla\cdot\left(-\left\langle p^{l;l}\right\rangle^{i}\mathbf{I}+\left\langle\boldsymbol{\tau}^{l;l}\right\rangle^{i}\right)\\
&\quad+\underbrace{\left(1-\delta_{kl}\right)K^{k;l}\left\{\left(\mathbf{u}^{l;l}-\mathbf{u}^{k;l}\right)+\frac{\overline{\alpha^{k;l}\mathbf{u}^{"l;l}}}{\alpha^{k;l}}\right\}}_{k\text{ is dispersed in }l}\\
&\quad+\underbrace{\delta_{kl}\sum_{j=1}^{L}K^{j;l}\left\{\left(\mathbf{u}^{j;l}-\mathbf{u}^{l;l}\right)-\frac{\overline{\alpha^{j;l}\mathbf{u}^{"l;l}}}{\alpha^{j;l}}\right\}}_{j\text{ is dispersed in }l}\\
&\quad\underbrace{-\left(1-\delta_{kl}\right)\frac{1}{\Delta V}\int_{A_{k;l\uparrow l;l}}\rho^{k;l}\mathbf{u}^{k;l}\left(\mathbf{u}^{k;l}-\mathbf{u}_{I,k;l\uparrow l;l}\right)\cdot\mathbf{n}_{k;l\uparrow l;l}dS}_{k\text{ is dispersed in }l}\\
&\quad\underbrace{-\delta_{kl}\frac{1}{\Delta V}\sum_{j=1}^{L}\int_{A_{l;l\uparrow j;l}}\rho^{l;l}\mathbf{u}^{l;l}\left(\mathbf{u}^{l;l}-\mathbf{u}_{I,l;l\uparrow j;l}\right)\cdot\mathbf{n}_{l;l\uparrow j;l}dS}_{j\text{ is dispersed in }l}
\end{aligned}
\tag{35}
$$

Here we again have used the Kronecker delta δ_{kl} to distinguish between dispersed and continuous fields. ΔV is the size of the control volume in which the areas $A_{k;l\uparrow l;l}$ and $A_{l;l\uparrow j;l}$ are defined. The LHS terms represent transient variation, stresses due to sub-cell mixing and convection. The RHS terms are external forces (gravity), fluid pressure and viscous stress, the two next groups of terms contain hydrodynamic drag and dispersion due to sub-volume mixing, and the last two groups of terms are momentum exchange due to mass transfer.

Extension to multiple continuous fields within a grid cell

Based on the generic averaging theorems ((Quintard and Whitaker, 1995), (Gray and Lee, 1977) and (Cushman, 1982)), the momentum equation for a continuous field is written as

$$
\begin{aligned}
&\frac{\partial}{\partial t}\int_{V^{l;l}}\rho^{l;l}\mathbf{u}^{l;l}dV=\int_{V^{l;l}}\rho^{l;l}\mathbf{g}dV+\int_{S^{l;l}}\left(-p^{l;l}\mathbf{I}+\boldsymbol{\tau}^{l;l}\right)\cdot\mathbf{n}^{l;l}dS\\
&\quad-\sum_{\substack{\text{All dispersed}\\ \text{fields k;l in l;l}}}\int_{A_{k;l\uparrow l;l}}\left(-p^{l;l}\mathbf{I}+\boldsymbol{\tau}^{l;l}\right)\cdot\mathbf{n}_{k;l\uparrow l;l}dS\\
&\quad\underbrace{-\sum_{\substack{\text{All continuous fields m;m,}\\ \text{interacting with l;l}}}\int_{A_{m;m\uparrow l;l}}\left(-p^{l;l}\mathbf{I}+\boldsymbol{\tau}^{l;l}\right)\cdot\mathbf{n}_{m;m\uparrow l;l}dS}_{LSI\_wall}\\
&\quad-\int_{S^{l;l}}\rho^{l;l}\mathbf{u}^{l;l}\mathbf{u}^{l;l}\cdot\mathbf{n}^{l;l}dS\\
&\quad-\sum_{\substack{\text{All other fields}\\ \text{inside volume}}}\int_{A_{k;l\uparrow l;l}}\rho^{k;l}\mathbf{u}^{k;l}\left(\mathbf{u}^{k;l}-\mathbf{u}_{I,k;l\uparrow l;l}\right)\cdot\mathbf{n}_{l;l\uparrow k;l}dS
\end{aligned}
\tag{36}
$$

All terms in Eq. (36) except one has been introduced through Eq. (35). The new term is marked with *LSI_wall* and represents the force acting at the large scale interface between two continuous fields. Shear and normal stresses at solid walls or LSIs are handled by this term, as these are stresses and pressures resolved on the scale of the control volume ΔV.

For now disregarding the interfacial pressure difference due to curvature, we may drop the pressure contributions acting inside the grid cell and assume that all phases share the same pressure. This simplification may lead to problems in certain cases and will be analysed at a later stage. At the LSI, as well as at solid walls, the jump condition for mass flow normal to the interface must always be fulfilled.

By application of the method discussed under the section "Treatment of wall boundary conditions" we may write the tangential LSI exchange force as

$$
\int_{A_{m;m\uparrow l;l}}\boldsymbol{\tau}^{l;l}\cdot\mathbf{n}_{m;m\uparrow l;l}dS_{m;m\uparrow l;l}\simeq\left(\boldsymbol{\tau}^{l;l}\right)_{m;m\uparrow l;l}\cdot\mathbf{n}_{m;m\uparrow l;l}\Delta S_{m;m\uparrow l;l}
\tag{37}
$$

This may further be linearized in the velocities; take for example the *x*-velocity component (ref. Eq. (26)), being expressed as

$$
F_{w,x}=-\tau_A n_{t,x}\Delta S_{m;m\uparrow l;l}-\chi n_{t,x}\left(u_x-u_{LSI,x}\right)\Delta S_{m;m\uparrow l;l},
\tag{38}
$$

which we generalize to

$$
\begin{aligned}
&\left(\boldsymbol{\tau}^{l;l}\right)_{m;m\uparrow l;l}\cdot\mathbf{n}_{m;m\uparrow l;l}\Delta S_{m;m\uparrow l;l}=\\
&\Theta_{m;m\uparrow l;l}+\Phi_{m;m\uparrow l;l}\left(\mathbf{u}_{m;m\uparrow l;l}-\mathbf{u}^{l;l}\right)
\end{aligned}
\tag{39}
$$

The coefficients $\Theta_{m;m\uparrow l;l}$ and $\Phi_{m;m\uparrow l;l}$ are defined by Eqs. (20) - (26). We may further note that for a solid wall, in Eq. (39) we will use $\mathbf{u}^{m;m}$ as the wall velocity. If the interface is moving, we must consider Newton's 3rd law. For each interface, we have the relation,

$$
\begin{aligned}
&\left(\boldsymbol{\tau}^{l;l}\right)_{m;m\uparrow l;l}\cdot\mathbf{n}_{m;m\uparrow l;l}\Delta S_{m;m\uparrow l;l}=\left(\boldsymbol{\tau}^{m;m}\right)_{l;l\uparrow m;m}\cdot\mathbf{n}_{l;l\uparrow m;m}\Delta S_{l;l\uparrow m;m}\\
&\qquad\Updownarrow\\
&\Theta_{m;m\uparrow l;l}+\Phi_{m;m\uparrow l;l}\left(\mathbf{u}_{m;m\uparrow l;l}-\mathbf{u}^{l;l}\right)=\\
&\qquad\Theta_{l;l\uparrow m;m}+\Phi_{l;l\uparrow m;m}\left(\mathbf{u}_{m;m\uparrow l;l}-\mathbf{u}^{m;m}\right)
\end{aligned}
\tag{40}
$$

which couples the two continuous fields over the interface.

As a result of Eq. (40), we obtain the interface velocity:

$$
\mathbf{u}_{m;m\uparrow l;l}=\frac{\Theta_{m;m\uparrow l;l}-\Theta_{l;l\uparrow m;m}+\left(\mathbf{u}^{m;m}\Phi_{l;l\uparrow m;m}-\mathbf{u}^{l;l}\Phi_{m;m\uparrow l;l}\right)}{\left(\Phi_{l;l\uparrow m;m}-\Phi_{m;m\uparrow l;l}\right)}
\tag{41}
$$

And, finally, for the exchange force, we get,

$$
\begin{aligned}
&\left(\boldsymbol{\tau}^{l;l}\right)_{m;m\uparrow l;l}\cdot\mathbf{n}_{m;m\uparrow l;l}\Delta S_{m;m\uparrow l;l}=\\
&\qquad\left(\frac{\Phi_{l;l\uparrow m;m}\Theta_{m;m\uparrow l;l}-\Phi_{m;m\uparrow l;l}\Theta_{l;l\uparrow m;m}}{\Phi_{l;l\uparrow m;m}-\Phi_{m;m\uparrow l;l}}\right)\\
&\qquad+\left(\frac{\Phi_{m;m\uparrow l;l}\Phi_{l;l\uparrow m;m}}{\Phi_{l;l\uparrow m;m}-\Phi_{m;m\uparrow l;l}}\right)\left(\mathbf{u}^{m;m}-\mathbf{u}^{l;l}\right)
\end{aligned}
\tag{42}
$$

The suggested method is ready for application of wall functions since the quantities entering into Eq. (38), like $n_{t,x}$, τ_A, and χ are readily computed from wall functions. As a result, the LSI forces acting on the field *k;l* is given by,

$$
\delta_{kl}\sum_{\substack{\text{All continuous fields m;m,}\\ \text{interacting with l;l}}}\left(\psi_{l;l\uparrow m;m}+\vartheta_{l;l\uparrow m;m}\left(\mathbf{u}^{m;m}-\mathbf{u}^{l;l}\right)\right),
\tag{43}
$$

where the coefficients are given by,

$$
\begin{aligned}
&\psi_{l;l\uparrow m;m}=\psi_{m;m\uparrow l;l}=\left(\frac{\Phi_{l;l\uparrow m;m}\Theta_{m;m\uparrow l;l}-\Phi_{m;m\uparrow l;l}\Theta_{l;l\uparrow m;m}}{\Phi_{l;l\uparrow m;m}-\Phi_{m;m\uparrow l;l}}\right)\\
&\vartheta_{l;l\uparrow m;m}=\vartheta_{m;m\uparrow l;l}=\left(\frac{\Phi_{m;m\uparrow l;l}\Phi_{l;l\uparrow m;m}}{\Phi_{l;l\uparrow m;m}-\Phi_{m;m\uparrow l;l}}\right)
\end{aligned}
\tag{44}
$$

Simplified model equations

Here we neglect molecular and mechanical mass transfer. Then the mass conservation equation (33) becomes:

$$
\frac{\partial\hat{\rho}_{\mathbf{i}}^{k;m}}{\partial t}\Delta V_{\mathbf{i}}+\sum_{\mathbf{k}\in\mathscr{F}_{\mathbf{i}}}\left(\hat{\rho}\,\mathbf{u}\cdot\mathbf{n}\,\Delta A\right)_{\mathbf{k}}=0
\tag{45}
$$

Similarly, the momentum equation in (35) is written

$$\frac{\partial}{\partial t}\left(\alpha^{k;l}\rho^{k;l}\mathbf{u}^{k;l}\right)+\nabla\cdot\left(\alpha^{k;l}\rho^{k;l}\mathbf{u}^{k;l}\mathbf{u}^{k;l}\right)=\alpha^{k;l}\rho^{k;l}\mathbf{g}+$$
$$\alpha^{k;l}\nabla\cdot\left(-\left\langle p^{l;l}\right\rangle^{i}\mathbf{I}+\left\langle\boldsymbol{\tau}^{l;l}\right\rangle^{i}\right)+\nabla\cdot\left(\alpha^{k;l}\rho^{k;l}\Gamma_{sub}{}^{k;l}\nabla\mathbf{u}^{k;l}\right)$$
$$+\underbrace{(1-\delta_{kl})K^{k;l}\left\{\left(\mathbf{u}^{l;l}-\mathbf{u}^{k;l}\right)+\left(\frac{\nu_t^{l;l}}{Sc_t^{l;l}}\frac{\nabla\overline{\alpha^{l;l}}}{\overline{\alpha^{l;l}}}-\frac{\nu_t^{l;l}}{Sc_t^{k;l}}\frac{\nabla\overline{\alpha^{k;l}}}{\overline{\alpha^{k;l}}}\right)\right\}}_{\text{k is dispersed in l}}\qquad(46)$$
$$+\underbrace{\delta_{kl}\sum_{j=1}^{L}K^{j;l}\left\{\left(\mathbf{u}^{j;l}-\mathbf{u}^{l;l}\right)-\left(\frac{\nu_t^{l;l}}{Sc_t^{l;l}}\frac{\nabla\overline{\alpha^{l;l}}}{\overline{\alpha^{l;l}}}-\frac{\nu_t^{l;l}}{Sc_t^{j;l}}\frac{\nabla\overline{\alpha^{j;l}}}{\overline{\alpha^{j;l}}}\right)\right\}}_{\text{j is dispersed in l}}$$
$$+\delta_{kl}\sum_{\substack{\text{All continuous fields m;m,}\\ \text{interacting with l;l}}}\left(\psi_{l;l\uparrow m;m}+\vartheta_{l;l\uparrow m;m}\left(\mathbf{u}^{m;m}-\mathbf{u}^{l;l}\right)\right)$$

Here, the last term contains all the large-scale interfaces (LSI) and fluid-solid wall stresses. This will work fine as long at the interface are located away from cell boundaries. For LSIs adjacent of coinciding with a cell boundary (will not be very frequent), the LSI exchange force will have to be modified. In the normal case, the exchange force in the Cartesian *x*-direction may look like:

$$\left(\psi_{l;l\uparrow m;m}+\vartheta_{l;l\uparrow m;m}\left(\mathbf{u}^{m;m}-\mathbf{u}^{l;l}\right)\right)\vec{\mathbf{e}}_x=A_L+B_L(u_L^{m;m}-u_L^{l;l})\qquad(47)$$

The index L is here the cell index. However, if the LSI is very close to the cell face *L-LYM* (LYM is neighbour on y^- side of the cell face) we will have to replace (47) with:

$$\left(\psi_{l;l\uparrow m;m}+\vartheta_{l;l\uparrow m;m}\left(\mathbf{u}^{m;m}-\mathbf{u}^{l;l}\right)\right)\vec{\mathbf{e}}_x=A_L+B_L(u_{LYM}^{m;m}-u_L^{l;l})\qquad(48)$$

In this case the computational stencil is slightly changed, as we have momentum exchange between two different fluids in two neighbouring computational cells.

We note that here the mixing stress term $\nabla\cdot\left(\alpha^{k;l}\rho^{k;l}\Gamma_{sub}{}^{k;l}\nabla\mathbf{u}^{k;l}\right)$ is simplified for the discussion purpose.

NUMERICAL DISCRETIZATION

Momentum equations

The momentum equation, disregarding mass transfer (Eq.(46)), may be reformulated into

$$\frac{\partial}{\partial t}\left(\hat{\rho}^{k;l}\mathbf{u}^{k;l}\right)+\nabla\cdot\left(\hat{\rho}^{k;l}\mathbf{u}^{k;l}\mathbf{u}^{k;l}\right)=\hat{\rho}^{k;l}\mathbf{g}$$
$$+\alpha^{k;l}\nabla\cdot\left(-\left\langle p^{l;l}\right\rangle^{i}\mathbf{I}+\left\langle\boldsymbol{\tau}^{l;l}\right\rangle^{i}\right)+\nabla\cdot\left(\hat{\rho}^{k;l}\Gamma_{sub}{}^{k;l}\nabla\mathbf{u}^{k;l}\right)$$
$$+(1-\delta_{kl})K^{k;l}\left(\mathbf{u}^{l;l}-\mathbf{u}^{k;l}\right)+\delta_{kl}\sum_{j=1}^{L}K^{j;l}\left(\mathbf{u}^{j;l}-\mathbf{u}^{l;l}\right)\qquad(49)$$
$$+\delta_{kl}\sum_{\substack{\text{All continuous fields m;m,}\\ \text{interacting with l;l}}}\left(\psi_{l;l\uparrow m;m}+\vartheta_{l;l\uparrow m;m}\left(\mathbf{u}^{m;m}-\mathbf{u}^{l;l}\right)\right)+\mathbf{S}^{k;l}$$

where the source term, assumed to be treated fully explicit, is given by:

$$\mathbf{S}^{k;l}=\underbrace{(1-\delta_{kl})K^{k;l}\left(\frac{\nu_t^{l;l}}{Sc_t^{l;l}}\frac{\nabla\overline{\alpha^{l;l}}}{\overline{\alpha^{l;l}}}-\frac{\nu_t^{l;l}}{Sc_t^{k;l}}\frac{\nabla\overline{\alpha^{k;l}}}{\overline{\alpha^{k;l}}}\right)}_{k\text{ is dispersed in }l}\qquad(50)$$
$$\underbrace{-\delta_{kl}\sum_{j=1}^{L}K^{j;l}\left(\frac{\nu_t^{l;l}}{Sc_t^{l;l}}\frac{\nabla\overline{\alpha^{l;l}}}{\overline{\alpha^{l;l}}}-\frac{\nu_t^{l;l}}{Sc_t^{j;l}}\frac{\nabla\overline{\alpha^{j;l}}}{\overline{\alpha^{j;l}}}\right)}_{j\text{ is dispersed in }l}$$

The terms of type $K^{k;l}(\mathbf{u}^{l;l}-\mathbf{u}^{k;l})$ and $K^{j;l}(\mathbf{u}^{j;l}-\mathbf{u}^{l;l})$ denotes friction between fields, and where we in the latter case sum over all fields *j*, dispersed in *k* = *l*.

As long as we can provide sub-models for the large-scale interface friction we may simulate any fluid-fluid, or fluid-solid system, allowing both direct simulations and more coarse-grained simulation possibilities.

The semi-discretized momentum equation for *k* in *l* now reads:

$$\hat{\rho}^{0,k;l}\frac{u_i^{k;l}-u_i^{0,k;l}}{\Delta t}$$
$$+\frac{\partial}{\partial x_j}\left(\hat{\rho}^{0,k;l}u_j^{0,k;l}u_i^{0,k;l}\right)-u_i^{0,k;l}\frac{\partial}{\partial x_j}\left(\hat{\rho}^{0,k;l}u_j^{0,k;l}\right)$$
$$=-\alpha^{0,k;l}\frac{\partial}{\partial x_i}p+\alpha^{0,k;l}\frac{\partial}{\partial x_j}\tau_{ji}^{k;l}+\frac{\partial}{\partial x_j}\left(\hat{\rho}^{k;l}\Gamma_{sub}^{k;l}\frac{\partial}{\partial x_j}u_i^{k;l}\right)\qquad(51)$$
$$+\sum_{m;n}\widehat{K}_{m;n}^{k;l}\left(u_i^{m;n}-u_i^{k;l}\right)+S_i^{0,k;l}$$

The drag force in (51) has been generalized by:

$$\sum_{m;n}\widehat{K}_{m;n}^{k;l}\left(\mathbf{u}^{m;n}-\mathbf{u}^{k;l}\right)\equiv(1-\delta_{kl})K^{k;l}\left(\mathbf{u}^{l;l}-\mathbf{u}^{k;l}\right)$$
$$+\delta_{kl}\sum_{j=1}^{L}K^{j;l}\left(\mathbf{u}^{j;l}-\mathbf{u}^{l;l}\right)\qquad(52)$$
$$+\delta_{kl}\sum_{\substack{\text{All continuous fields m;m,}\\ \text{interacting with l;l}}}\left(\psi_{l;l\uparrow m;m}+\vartheta_{l;l\uparrow m;m}\left(\mathbf{u}^{m;m}-\mathbf{u}^{l;l}\right)\right)$$

We may note that $\widehat{K}_{m;n}^{k;l}$ is defined by equations (47) and (52). For now we have not included the special cases for the LSI or wall perfectly aligned with the computational cell face, here represented by Eq. (48).

Similar to how we proceed for single phase flow, we first do a predictor step where we use explicit operators for all terms except for diffusion terms, which are solved implicitly. I.e., we use the momentum equation on the form,

$$\hat{\rho}^{0,k;l}\frac{u_i^{*,k;l}-u_i^{0,k;l}}{\Delta t}$$
$$+\frac{\partial}{\partial x_j}\left(\hat{\rho}^{0,k;l}u_j^{0,k;l}u_i^{0,k;l}\right)-u_i^{0,k;l}\frac{\partial}{\partial x_j}\left(\hat{\rho}^{0,k;l}u_j^{0,k;l}\right)$$
$$=-\alpha^{0,k;l}\frac{\partial}{\partial x_i}p^0+\alpha^{0,k;l}\frac{\partial}{\partial x_j}\tau_{ji}^{k;l}(\mathbf{u}^*)\qquad(53)$$
$$+\frac{\partial}{\partial x_j}\left(\hat{\rho}^{k;l}\Gamma_{sub}{}^{k;l}\frac{\partial}{\partial x_j}u_i^{*,k;l}\right)$$
$$+\sum_{m;n}\widehat{K}_{m;n}^{k;l}\left(u_i^{0,m;n}-u_i^{0,k;l}\right)+S_i^{0,k;l}$$

As external forces, friction, stress and pressure gradient balance out by large, the explicit friction term is included. By subtracting (53) from (51) we obtain:

$$
\begin{aligned}
&\hat{\rho}^{0,k;l}\frac{u_i^{k;l}-u_i^{*,k;l}}{\Delta t}\\
&= -\alpha^{0,k;l}\frac{\partial}{\partial x_i}\left(p-p^0\right)+\cancel{\alpha^{0,k;l}\frac{\partial}{\partial x_j}\left(\tau_{ji}^{k;l}-\tau_{ji}^{k;l}(\mathbf{U}^*)\right)}\\
&+\cancel{\frac{\partial}{\partial x_j}\left(\hat{\rho}^{k;l}\Gamma_{sub}^{k;l}\frac{\partial}{\partial x_j}\left(u_i^{k;l}-u_i^{*,k;l}\right)\right)}\\
&+\sum_{m;n}\widehat{K}_{m;n}^{k;l}\left(u_i^{m;n}-u_i^{k;l}-u_i^{0,m;n}+u_i^{0,k;l}\right)
\end{aligned}
\tag{54}
$$

The crossed-out terms are neglected at this stage of the algorithm following the reasoning behind the fractional step approach, i.e., the diffusion terms are completed in the predictor step, and do not carry over to the corrector step. This essentially introduces a first order error in time, however, for most practical purposes it performs almost as well a second order methods (LeVeque, 2007). When neglecting the crossed-out term in equation (54) we find that:

$$
\begin{aligned}
&u_i^{k;l}-K_{m;n}^{k;l}\frac{\Delta t}{\hat{\rho}^{0,k;l}}\left(u^{m;n}-u^{k;l}\right)\\
&=u_i^{*,k;l}-K_{m;n}^{k;l}\frac{\Delta t}{\hat{\rho}^{0,k;l}}\left(u^{0,m;n}-u^{0,k;l}\right)-\alpha^{0,k;l}\frac{\Delta t}{\hat{\rho}^{0,k;l}}\frac{\partial}{\partial x_i}p'
\end{aligned}
\tag{55}
$$

Here we assume the summing convention for the terms involving $K_{m;n}^{k;l}$. We recognize that Eq. (55) may be written on matrix form as

$$
\mathbf{A}\mathbf{u}=\mathbf{b}-\Delta t\,\mathbf{a}\frac{\partial p'}{\partial x_i} \tag{56}
$$

where

$$
\mathbf{a}=\begin{bmatrix}\vdots\\ \alpha^{0,k;l}/\hat{\rho}^{0,k;l}\\ \vdots\end{bmatrix} \tag{57}
$$

and

$$
\mathbf{b}=\begin{bmatrix}\vdots\\ u_i^{*,k;l}-K_{m;n}^{k;l}\frac{\Delta t}{\hat{\rho}^{0,k;l}}\left(u^{0,m;n}-u^{0,k;l}\right)\\ \vdots\end{bmatrix} \tag{58}
$$

So the solution for the velocities may be written as,

$$
\mathbf{u}=\mathbf{A}^{-1}\mathbf{b}-\Delta t\,\mathbf{A}^{-1}\mathbf{a}\frac{\partial p'}{\partial x_i} \tag{59}
$$

Note that since we have used an explicit operator for the convective terms, and used the fractional step approach for diffusion terms, the matrix **A** only couples terms within a single grid cell. In a two-phase flow with 4 fields **A** is a 4×4 matrix, in three-phase flows we have a 9×9 matrix. If we had carried over the implicit diffusion operator from the predictor step, or used an implicit scheme for convection, the matrix **A** would also need to couple to the neighbouring cells, which we want to avoid. I.e., in the present approach, except for the diffusion operators of the predictor, there is no need for solving global matrices, which is a large benefit in terms of potential for achieving good parallel performance of the simulation code.

The main reason why we do not treat all terms explicitly, and dispose of the coupling matrix **A** altogether is that the terms coupling the field velocities within a cell can be quite stiff. Linearizing and coupling through the matrix **A** has been seen to be sufficient for stability.

Obtaining a pressure equation

To derive an equation for pressure, we use the volume constraint given in Eq. (34), which we may restate in terms of field masses $\hat{\rho}^{k;m}$ and densities $\rho^{k;m}$ as

$$
\sum_{m=1}^{N_{\text{phases}}}\sum_{k=1}^{N_{\text{phases}}}\Upsilon^{k;\mathrm{m}}\frac{\hat{\rho}_{\mathbf{i}}^{k;m}}{\rho_{\mathbf{i}}^{k;m}}=1 \tag{60}
$$

Note that Eq. (60) is also valid for single phase N_{phases}=1, where it will express that the density transported by the mass equation must equal the density determined by the equation of state.

The same is true for multiphase. Eq. (60) states that the cell masses must satisfy the thermodynamic relations so that the cell volume is exactly filled. Conceptually, in the corrector step of the algorithm we want to find a pressure that projects the solution onto the volume conserving manifold.

We start out by substituting for the masses from the solution of the mass equation (33). The mass equation can be reformulated as,

$$
\hat{\rho}_{\mathbf{i}}^{k;m}=\left(\hat{\rho}_{\mathbf{i}}^{k;m}\right)^0-\frac{\Delta t}{\Delta V_{\mathbf{i}}}\sum_{\mathbf{k}\in\mathscr{F}_{\mathbf{i}}}\left(\left(\hat{\rho}^{k,m}\right)^0\mathbf{u}^{k;m}\cdot\mathbf{n}\,\Delta A\right)_{\mathbf{k}}+\Delta t\;S_{\mathbf{i}}^{k;m} \tag{61}
$$

where masses are explicit and velocities implicit in the convection term. We want to use an explicit scheme for masses to keep numerical diffusion low, but we need the implicit velocities since they will be adjusted by the pressure, allowing for a volume consistent solution.

Now defining,

$$
\mathbf{u}^{**}=\mathbf{A}^{-1}\mathbf{b}\qquad\text{and}\qquad\mathbf{u}'=\mathbf{u}-\mathbf{u}^{**} \tag{62}
$$

we may rewrite Eq. (59) as,

$$
\mathbf{u}'=-\Delta t\mathbf{A}^{-1}\mathbf{a}\frac{\partial p'}{\partial x_i} \tag{63}
$$

which we on component form write as,

$$
\left(u_i^{k;m}\right)'=-DU^{k;m}\frac{\partial p'}{\partial x_i}\,. \tag{64}
$$

where $DU_i^{k;m}$ is the element in the vector preceding the pressure gradient in Eq. (63) that correspond to the velocity $u_i^{k;m}$. For the velocities normal to the cell faces in Eq. (61), we may then write

$$
\mathbf{u}^{k;m}\cdot\mathbf{n}=\left(\mathbf{u}^{k;m}\right)^{**}\cdot\mathbf{n}-DU^{k;m}\nabla p'\cdot\mathbf{n}\,. \tag{65}
$$

Further, defining a predicted field mass as,

$$
\begin{aligned}
\left(\hat{\rho}_{\mathbf{i}}^{k;m}\right)^{**}&=\left(\hat{\rho}_{\mathbf{i}}^{k;m}\right)^0\\
&-\frac{\Delta t}{\Delta V_{\mathbf{i}}}\sum_{\mathbf{k}\in\mathscr{F}_{\mathbf{i}}}\left(\left(\hat{\rho}^{k,m}\right)^0\left(\left(\mathbf{u}^{k;m}\right)^{**}\cdot\mathbf{n}\right)\Delta A\right)_{\mathbf{k}}+\Delta t\;S_{\mathbf{i}}^{k;m}
\end{aligned}
\tag{66}
$$

we may write the mass equation (61) as

$$
\hat{\rho}_{\mathbf{i}}^{k;m}=\left(\hat{\rho}_{\mathbf{i}}^{k;m}\right)^{**}+\frac{\Delta t}{\Delta V_{\mathbf{i}}}\sum_{\mathbf{k}\in\mathscr{F}_{\mathbf{i}}}\left(\left(\hat{\rho}^{k,m}\right)^0\left(DU^{k;m}\nabla p'\cdot\mathbf{n}\right)\Delta A\right)_{\mathbf{k}} \tag{67}
$$

Substituting Eq. (67) into the volume constraint, we get the pressure equation

$$
\begin{aligned}
&\sum_{m=1}^{N_{\text{phases}}}\sum_{k=1}^{N_{\text{phases}}}\Upsilon^{k;\mathrm{m}}\frac{\frac{\Delta t}{\Delta V_{\mathbf{i}}}\sum_{\mathbf{k}\in\mathscr{F}_{\mathbf{i}}}\left(\left(\hat{\rho}^{k,m}\right)^0\left(DU^{k;m}\nabla p'\cdot\mathbf{n}\right)\Delta A\right)_{\mathbf{k}}}{\rho_{\mathbf{i}}^{k;m}}=\\
&1-\sum_{m=1}^{N_{\text{phases}}}\sum_{k=1}^{N_{\text{phases}}}\Upsilon^{k;\mathrm{m}}\frac{\left(\hat{\rho}_{\mathbf{i}}^{k;m}\right)^{**}}{\rho_{\mathbf{i}}^{k;m}}
\end{aligned}
\tag{68}
$$

where we recognize the right-hand side of the equation as the volume error in the predicted masses. We have not discussed the details of the discretization of the gradient of the pressure correction, but essentially, the left hand side of Eq. (68) will be a weighed discrete Laplace operator for the pressure correction.

Note that for constant densities, Eq. (68) is a linear equation for pressure, i.e., after solving the equation we will get a velocity field and masses that exactly satisfies the volume constraint.

However, generally the density will be a function of pressure. I.e., taking the thermodynamics into account makes Eq. (68) non-linear, and we may need to iterate on the pressure equation to satisfy the volume constraint to some specified tolerance. To improve convergence, we linearize the equation in pressure, essentially getting a Newton iteration for pressure. Experience shows that this iteration indeed exhibit quadratic convergence. Note also that we iterate only on the pressure equation, only updating density, velocities, and masses $\left(\hat{\rho}_{\mathbf{i}}^{k;m}\right)^{**}$ between each iteration.

Linearizing the pressure equation in pressure, we get,

$$-\chi_p p'_{\mathbf{i}} + \sum_{m=1}^{N_{\text{phases}}}\sum_{k=1}^{N_{\text{phases}}} \Upsilon^{k;\text{m}} \frac{\dfrac{\Delta t}{\Delta V_{\mathbf{i}}}\sum_{\mathbf{k}\in\mathscr{F}_{\mathbf{i}}}\left(\left(\hat{\rho}^{k,m}\right)^0\left(DU^{k;m}\nabla p'\cdot\mathbf{n}\right)\Delta A\right)_{\mathbf{k}}}{\rho_{\mathbf{i}}^{k;m}} = 1-\sum_{m=1}^{N_{\text{phases}}}\sum_{k=1}^{N_{\text{phases}}}\Upsilon^{k;\text{m}}\frac{\left(\hat{\rho}_{\mathbf{i}}^{k;m}\right)^{**}}{\rho_{\mathbf{i}}^{k;m}} \quad (69)$$

where χ_p is the multiphase compressibility factor,

$$\chi_p = \sum_{m=1}^{N_{\text{phases}}}\sum_{k=1}^{N_{\text{phases}}}\Upsilon^{k;\text{m}}\frac{\alpha_{\mathbf{i}}^{k;m}}{\rho_{\mathbf{i}}^{k;m}}\frac{\partial\rho^{k;m}}{\partial p}\bigg|_{\mathbf{i}} \quad (70)$$

Finally, we may note that since the updated velocities are always inserted into Eq. (61), mass will always be conserved. The error we may have is a deviation from the volume constraint. However, since the volume error is the driving term at right hand side of Eq. (69), and it is at all time based on the latest estimate of cell masses, the solution will always relax towards the solution manifold where the volume constraint is satisfied.

The solution procedure

1) Prediction of extensive densities, by Eq. (66).
2) A first prediction of the phase velocities, Eq. (53). Here the stress terms are treated implicitly.
3) Establishing the momentum exchange matrix coefficients, equation (55) and (56), for the final momentum equation.
4) Computing inverse of the **A** matrix for each grid cell, Eq. (56).
5) Establish the coefficients in the relation between final velocity and pressure update gradient, Eq. (64)
6) By using the pressure correction (update) equation (69), compute the pressure correction $p' = p - p^0$.
7) Update pressures.
8) Update all field velocities, Eq. (65).
9) Update extensive phase densities, Eq. (67).
10) Update thermodynamic properties, in particular densities, based on new pressures (and temperatures if the energy equation is solved for).
11) Recalculate the right-hand side of the pressure equation (69) using new extensive densities and field densities, i.e., calculate the volume error for the solution.
12) If the volume error is greater than some tolerance, go to 6).
13) Advance to next time step

Note that no iterations are needed, except possibly for the pressure equation to reduce volume error. Our preliminary testing indicates, however, that most of the time no iterations are needed. Further, the iterations exhibit quadratic convergence, so only one or maybe two iterations are always sufficient.

DISCUSSION

The method described above has this far only been implemented and validated for single phase, including moving walls. In these laminar flow test cases good results have been obtained, and will be presented in a separate publication (Dang, S. T. et al., 2017). In the general case of multiple moving materials we need a reliable method to compute interface propagation and at the same time provide the geometric information needed to handle the flow in the cut cells. The most promising strategy here seems to be the level-Set-VOF method (Chakraborty et al., 2013). As probably noted by the reader, the discretization schemes for convection has not been discussed in detail. SIMCOFLOW will however be open to plugging in any scheme which is supported by the code infrastructure. In the case of an octree grid we may not allow the use of large grid stencils for interpolation.

The method proposed herein will not need gridding in the way we normally do. The entire geometry is placed inside a cube and a regular Cartesian grid is established based on a surface geometry file (STL format). Based on this a level set function is established, describing the initial geometry.

Adaptive grid refinement is being allowed, using an octree grid arrangement. However, the code may run with or without adaptive grids. An important design element here is that all the moving interfaces will be on the same grid level during one time step to facilitate high accuracy and ease of implementation of boundary and interface phenomena.

The SIMCOFLOW code is being designed for parallel execution.

The results of this work will be published under a GNU Open Source licence.

CONCLUSIONS

A method to simulate generic multi material flows in a Cartesian framework, using a staggered grid arrangement, is proposed.

The method is using Cartesian cut-cells, where the volume fractions in grid cells, or the value of the level set function, describe the positions of the materials inside the system.

The method is capable of simulating any number of flowing fluids, containing dispersed fields. Here the dispersed fields may be entrained from or deposit on the large scale interfaces.

The proposed method allows to use detailed boundary conditions, for all fields represented, at the large scale interfaces.

Introduction of floating objects such as boys and vessels will be easy to integrate if these are described by a level set function.

ACKNOWLEDGEMENTS

The Norwegian Research Council, through the researcher program SIMCOFLOW (proj. 234126), is acknowledged for supporting this work.

REFERENCES

Chakraborty, I., Biswas, G., Ghoshdastidar, P.S., 2013. A coupled level-set and volume-of-fluid method for the buoyant rise of gas bubbles in liquids. Int. J. Heat Mass Transf. 58, 240–259.

Cheny, Y., Botella, O., 2010. The LS-STAG method: A new immersed boundary/level-set method for the computation of incompressible viscous flows in complex moving geometries with good conservation properties. J. Comput. Phys. 229, 1043–1076.

Cushman, J.H., 1982. Proofs of the volume averaging theorems for multiphase flow. Adv. Water Resour. 5, 248–253.

Dang, S. T., Johansen, S.T., Meese, E. A., 2017. A Cartesian cut-cell method based on formal volume averaging of mass momentum and energy equations. Presented at the CFD2017, SINTEF Proceedings, Trondheim.

Gray, W.G., Lee, P.C.Y., 1977. On the theorems for local volume averaging of multiphase systems. Int. J. Multiph. Flow 3, 333–340.

Hirt, C.W., Sicilian, J.M., 1985. A porosity technique for the definition of obstacles in rectangular cell meshes (Flow Science Inc.). New Mexico.

Johansen, S.T., Laux, H., 1995. An alternative method for numerical solution of dispersed multiphase flow equations. Presented at the The 2nd International Conference on Multiphase Flow ’95 Kyoto, April 3 -7, p. NU 8.

Laux, H., Meese, E., Johansen, S.T., Ladam, Y., Bansal, K.A., Danielson, T.J., Goldszal, A., Monsen, J.I., 2007. Simulation of multiphase flows composed of large scale interfaces and dispersed fields. Proc. ICMF 2007 Leipz.

LeVeque, R.J., 2007. Finite volume methods for hyperbolic problems, 6th ed. Cambridge University Press.

Quintard, M., Whitaker, S., 1995. Aerosol filtration: An analysis using the method of volume averaging. J Aerosol Sci 26, 1227–1255.